Journal of the Brazilian Society of Mechanical Sciences and Engineering (2024) 46:424
https://doi.org/10.1007/s40430-024-04999-4

TECHNICAL PAPER

Effect of heat treatment parameters on microstructure and microhardness of 15-5PH stainless steel fabricated by selective laser melting

Asma Mansoura[1] · Shayan Dehghan[1] · Noureddine Barka[1] · Sasan Sattarpanah Karganroudi[2] · Manel Houria[3]

Received: 20 December 2023 / Accepted: 21 May 2024 / Published online: 4 June 2024

Abstract
Selective laser melting (SLM) is an advanced additive manufacturing technology that creates complex geometries that were previously impossible to produce. However, for industrial applications that require the highest standards, the performance of SLM-manufactured metal components still needs to be improved. Therefore, post-processing heat treatment is necessary to enhance additively manufactured parts' microstructural and mechanical properties. The 15-5PH stainless steel is a precipitation-hardenable stainless steel with excellent corrosion resistance, strength, and hardness. This study aims to optimize the precipitation hardening heat treatment parameters for 15-5PH stainless steel produced by SLM. The factors considered in this study are the quenching solution, aging temperature, and aging time, with three levels for each factor. The microstructure of samples is analyzed using Optical Microscopy and Scanning Electron Microscopy to understand the relationship between microstructure and properties. The analysis of variance (ANOVA) is also used to assess the primary effect of each heat treatment factor. The presence of uniformly distributed fine Cu precipitates results in the highest hardness after aging at 500 °C for 1 h. The results also show that aging temperature is the most significant parameter for part hardness, while the quenching solution has no effect. The proposed method developed a reliable regression model that accurately predicts the hardness of heat-treated 15-5PH stainless steel manufactured by SLM as a function of aging temperature and aging time. Validation experiments demonstrate that optimizing precipitation hardening parameters may also improve tensile strength and ductility.

Keywords Selective laser melting · Precipitation hardening · 15-5PH stainless steel · ANOVA · Microhardness

1 Introduction

The development of additive manufacturing technologies has allowed the industry to overcome constraints associated with conventional techniques [1]. As a single-step process, the primary advantages of AM include freedom of design, energy and material savings, and shortened design-to-manufacture time [2]. One of the most promising metal additive manufacturing processes is SLM, a laser powder-bed fusion process (LPBF) that uses a scanning laser beam to build up parts by selectively melting certain portions of the metal powder-bed, layer by layer, based on computer-aided design (CAD) data. SLM is increasingly popular because of its ability to process a wide variety of materials, including those that are expensive or difficult to produce, using traditional techniques such as steel, aluminum alloys, titanium alloys, and nickel alloys [3]. In addition, this technology provides the opportunity to enhance functionality and customize the microstructure and subsequent properties of the manufactured part [4].

Despite the numerous benefits of SLM, the industry still faces challenges in fully accepting it. The presence of defects such as porosity, lack of fusion, cracks, anisotropy, inhomogeneous microstructure, and high residual stress makes it a

Technical Editor: Henara Lillian Costa.

✉ Shayan Dehghan
shayan.dehghan@uqar.ca

[1] Department of Mathematics, Computer Science and Engineering, University of Quebec at Rimouski, Rimouski, Quebec QC G5L 3A1, Canada

[2] Department of Mechanical Engineering, University of Quebec at Trois-Rivières, Trois-Rivières, Quebec QC G8Z 4M3, Canada

[3] Department of Mechanical Engineering, Ecole de Technologie Superieure (ÉTS), Montreal QC H3C 1K3, Canada

complicated process. The complex thermal history and rapid cooling rate are the main reasons behind these issues [5, 6].

15-5PH stainless steel is a martensitic precipitation hardening stainless steel with high corrosion resistance, good toughness, and good mechanical properties at temperatures up to 300 °C [7, 8]. This makes it suitable for various aerospace, chemical, petrochemical, and food processing applications [9]. Due to the low carbon content and the addition of copper as an alloying element, its body-centered cubic (BCC) martensite matrix can be strengthened through the formation of nanometric-sized Cu precipitates [10, 11]. The conventional heat treatment for this type of alloy consists of two steps: (1) solution treatment in the austenite phase field, followed by air or water quenching; (2) aging in a heat treatment furnace at 480–620 °C for a few minutes to several hours [12]. Aging starts with forming small and coherent Cu clusters with a BCC structure. With increasing aging temperature and/or aging time, the precipitate size and shape evolve until they transform into incoherent face-centered cubic (FCC) clusters [13, 14]. By selecting proper post-process parameters, the characteristics of this precipitation in terms of volume fraction and size can be tuned to obtain different application-oriented mechanical properties [15, 16]. This combination of characteristics and high-value applications makes the 15-5PH stainless steel an excellent candidate for additive manufacturing. Recently, SLM has shown promising results for fabricating precipitation hardening stainless steels [17, 18]. Several studies have focused on comparing the performance of SLM-processed 15-5PH and traditionally manufactured 15-5PH stainless steel. Coffy et al. [19] reported a smaller grain size with a layered microstructure and a significant volume fraction of retained austenite phase in SLM-processed 15-5PH compared to the conventional alloy. Their study focused on martensite/austenite phase fractions and did not address mechanical properties. Roberts et al. [20] compared the microstructure, microhardness, and high-temperature mechanical behavior of AM and wrought 15-5PH steel in the as-built condition. According to their preliminary results, additively manufactured 15-5PH showed better performance except for ductility. However, further testing and investigations are needed. Some researchers investigated the effect of processing parameters such as energy density, scanning strategy, building direction, and powder characteristics on the microstructure and mechanical properties of selective laser-melted 15-5PH to obtain high-quality final parts [21–24]. However, this approach cannot effectively control anisotropy and heterogeneous microstructure caused by the complex metallurgical interactions during the SLM process, especially for precipitation hardening grade. Recent studies focused on post-process heat treatment to address this challenge to achieve a better tradeoff between microstructure and mechanical properties for 15-5PH stainless steel [9]. Nong et al. [25] examined the effect of the standard precipitation hardening heat treatment H900 (i.e., solution heat treatment at 1040 °C for 30 min, followed by water quenching and subsequent aging at 482 °C for 1 h, followed by air-cooling) on the microstructural and mechanical characteristics of SLM-fabricated 15-5PH parts. They reported that the heat-treated SLM sample demonstrated greater strength and higher hardness than the aged wrought 15-5PH sample and comparable ductility. The finer grain structure, the high concentration of dislocations around grain boundaries, and the retained austenite explained this. Mechanical properties, microstructural evolution, and corrosion resistance were evaluated in several conditions (solution annealed, aged at different temperatures and times) [26–29]. Experimental results showed that different aging processes affect the Cu-rich precipitate characteristics and the amount of retained austenite, resulting in different mechanical behavior and corrosion resistance. These studies focused on standard heat treatments mainly designed for conventionally manufactured PH SS. A large dispersion of the mechanical property values is observed due to the high variability in phase composition and phase fractions of SLM-processed PH SSs. Thus, specific optimized heat treatment should be developed. Alafaghani et al. [9] investigated the influence of different solution annealing treatments on the microstructure and mechanical properties of SLM 15-5PH steel. They found that extending the solution treatment time improved microstructure isotropy and tensile strength at the expense of ductility, while increasing the solution treatment temperature adversely affected SLM parts. However, simple correlations drawn from experimental results without systematic analysis would not be effective for heat treatment optimization. Moreover, other parameters such as cooling rate, aging temperature, and aging time, outside the standard range were not yet investigated.

Therefore, it is necessary to conduct a comprehensive study on the effect of heat treatment parameters on the microstructure of SLM 15-5PH. The wide application of 15-5PH in different industries highlights the need for more research. To obtain the desired mechanical properties, it is essential to systematically identify optimal heat treatment parameters using efficient experimental design and analysis methods. The Taguchi method is a statistical experiment that optimizes designs for performance, quality, and cost [30].

Therefore, the main contribution of this research is to provide detailed insights into the heat treatment of 15-5PH fabricated through SLM and improve its microstructural and mechanical properties. This study aims to investigate the influence of precipitation hardening heat treatment parameters on the microstructure and microhardness of 15-5PH parts processed by SLM based on Taguchi's design. A statistical approach based on ANOVA, RSM, and linear regression has been utilized to identify the significant heat treatment parameters and predict their effects on 15-5PH

microhardness. Additionally, microstructure characterization has been performed and correlated to the obtained hardness.

The findings for this work are expected to develop the application range of SLM 15-5PH in different industries where the properties enhancement of material is necessary.

2 Material and methods

2.1 Design of experiment

The Taguchi method is a simple and powerful optimization tool to evaluate the significance of different process parameters for a target response. It allows reducing the number and cost of experimental tests without affecting accuracy, thanks to the orthogonal array design [31]. The procedure of Taguchi design includes the following steps: (1) identification of the quality characteristics and selection of the design parameters; (2) selection of the appropriate orthogonal array according to the number of parameters and number of levels; (3) conduction of the experiments and statistical analysis of the results; and (4) identification of the optimal levels of design parameters [30].

The microhardness of precipitation hardening stainless steel relies on a complex microstructure developed during a quenching sequence after austenitization, followed by aging heat treatment [10]. Aging temperature and aging time play a prominent role in controlling the Cu precipitate characteristics and, thus, the alloy's strength. The homogenization step and the subsequent quench are also crucial in the control of austenite/martensite proportions. Accordingly, quenching solution (A), aging temperature (B), and aging time (C) are selected as design parameters for the Taguchi plan. Three levels for each parameter are set, as shown in Table 1.

For conventional 15-5PH, a solution heat treatment is typically applied in the austenitic domain (~ 1050 °C), followed by quenching, to obtain a fully martensitic structure. A subsequent aging treatment in the range of 480–620 °C is conducted for 1–4 h, which results in precipitation hardening by copper precipitates. Precipitation begins with small and coherent spherical Cu clusters with a BCC structure, which transform into an elliptical incoherent FCC structure, called ε-Cu, upon over-aging [13].

Aging parameters were chosen to cover the typical under-aged, peak-aged, and over-aged conditions known in standard precipitation hardening treatments while exploring a lower range of temperature and time to reduce post-processing cost and time. For quenching, three different aqueous solutions were used in the experiments: distilled water (S1), NaCl solution at 6% of mass concentration (S2), and 12 mass% NaCl solution (S3), allowing three different quenching rates as reported in [32]. Based on the Taguchi method, the appropriate experimental design for this study is an L9 orthogonal array. This array has eight degrees of freedom and, thus, is suitable for three-level design parameters. Therefore, nine unique heat treatment combinations are available, as shown in Table 2. Overall, parameters' levels are determined to balance the need for precision and the practical limitations of the experiment, taking into account prior knowledge and experience.

Table 1 Heat treatment parameters and their levels

Parameters	Symbols	Levels		
Quenching solution	A	S1	S2	S3
Aging temperature (°C)	B	400	500	600
Aging time (min)	C	60	120	180

2.2 Specimen fabrication and preparation

The samples were produced on the EOS M 290 system using the commercialized PowderRange 155 stainless steel (15-5PH) powder from Carpenter Additive. The particle size distribution ranges from 15 to 45 µm. Table 3 lists the chemical composition of the 15-5PH powder used.

The SLM machine has a Yb-fiber laser with a beam diameter of 0.1 mm. To avoid oxidation, printing was done in an argon atmosphere. Specimens were produced using optimized processing parameters recommended by the manufacturer, which are listed in Table 4. Figure 1 depicts the dimensions and building orientation of the specimen. Laser scan paths were rotated at a 45° angle between two adjacent layers. It is worth noting that both the substrate and tensile samples were made of 15-5PH. After the builds were completed, tensile samples were separated from the substrate using a wire EDM machine and then sandblasted to homogenize surfaces.

Table 2 Experimental layout using L9 orthogonal array

Samples	Quenching solution	Aging temperature (°C)	Aging time [min]
	A	B	C
S1-400 °C-60 min	1	400	60
S1-500 °C-120 min	1	500	120
S1-600 °C-180 min	1	600	180
S2-400 °C-120 min	2	400	120
S2-500 °C-180 min	2	500	180
S2-600 °C-60 min	2	600	60
S3-400 °C-180 min	3	400	180
S3-500 °C-60 min	3	500	60
S3-600 °C-120 min	3	600	120

Table 3 Chemical composition of 15-5PH stainless steel powder (wt%)

Element	C	Cr	Cu	Fe	Mn	Ni	Nb	N	O	P	Si	S
wt%	≤0.04	14.0–14.6	3.5–4.0	Bal	≤0.3	2.8–4.5	0.20–0.40	≤0.1	≤0.03	≤0.03	≤0.7	≤0.03

Table 4 SLM process parameters for 15-5PH stainless steel

Parameter	Laser power (W)	Scan speed (mm/s)	Hatch spacing (mm)	Layer thickness (μm)
Value	195	800	0.1	40

For comparison, we kept two samples in their as-built condition. In the first step, the remaining samples were solution-treated at 1020 °C for 15 min. Each group of three is then cooled in a different quenching solution (1, 2, and 3). After quenching, samples are individually aged in the furnace at different temperatures and holding durations according to the orthogonal array (see Table 2) and cooled in air, giving rise to precipitation hardening. Two other validation samples were later solution-treated at 1020 °C for 15 min, water-quenched, and aged in a furnace according to the optimal set of parameters.

2.3 Microstructure, microhardness, and tensile tests

To evaluate the microhardness and microstructure of SLM-fabricated 15-5PH steel samples at their cross-section parallel to the building direction, samples were mounted in epoxy and polished with diamond suspensions with average diamond particle diameters of 9 μm, 6 μm, 3 μm, and 1 μm. The samples were then chemically etched with Fry's reagent (5 g CuCl2 + 40 mL HCl + 30 mL water + 25 mL ethanol) to reveal grain structure. Microstructure characterization was performed using LEXT OLS4100 laser confocal microscope, Hitachi TM3000 scanning electron microscope (SEM), and energy-dispersive spectroscopy (EDS). Vickers microhardness measurements were taken with a testing load

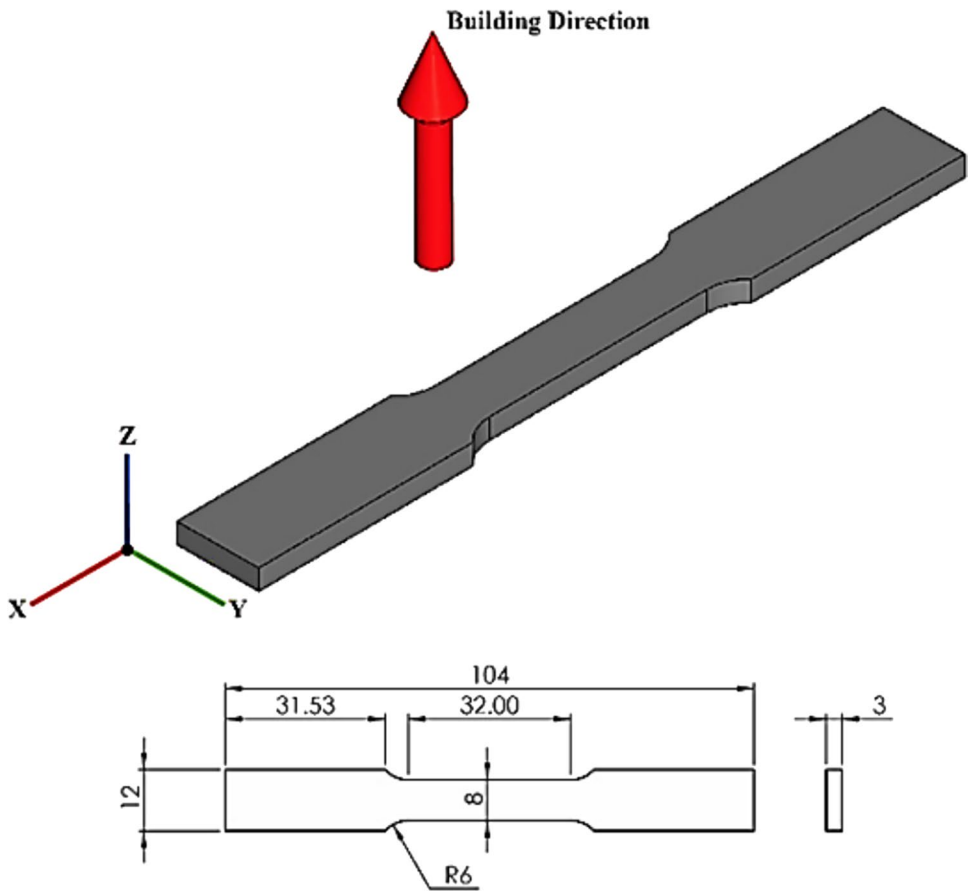

Fig. 1 Dimensions (in mm) and building direction of samples

of 300 gf and 10 s of dwell time using a Clemex machine, conforming to ASTM E384 standard. Values are automatically converted to Rockwell C by Clemex software based on ISO 18265 standard. For each sample, the hardness value is determined by averaging 20 indentations spaced at 200 µm and performed along the surface's diagonal.

After collecting experimental data, ANOVA and RSM were performed using Minitab 19 statistical analysis software to determine significant heat treatment parameters and identify optimal parameters combination, respectively.

Room-temperature tensile tests were carried out on rectangular cross-section specimens (6×3 mm) with a 25mm gauge length using an MTS-810 tensile testing machine according to ASTM-E8 standards. An extensometer measured the elongation of the tensile specimens during testing.

Table 5 Microhardness test results

Sample	Factors			Response
	A	B	C	H (HRC)
S1-400 °C-60 min	1	400	60	40.0 ± 0.7
S1-500 °C-120 min	1	500	120	46.3 ± 0.8
S1-600 °C-180 min	1	600	180	36.8 ± 0.8
S2-400 °C-120 min	2	400	120	39.5 ± 1.3
S2-500 °C-180 min	2	500	180	44.2 ± 0.8
S2-600 °C-60 min	2	600	60	38.1 ± 0.7
S3-400 °C-180 min	3	400	180	38.9 ± 1.2
S3-500 °C-60 min	3	500	60	46.5 ± 0.7
S3-600 °C-120 min	3	600	120	37.1 ± 0.6
As-built	–	–	–	39.5 ± 0.6
S1-quenched	1	–	–	37.0 ± 0.8
S2-quenched	2	–	–	36.3 ± 1.0
S3-quenched	3	–	–	36.6 ± 0.6

Two samples for each of the as-built and optimal heat-treated conditions are tested.

3 Results and discussion

3.1 Microstructure analysis

The complex thermal cycle in the SLM process and subsequent heat treatments induce a complex microstructural evolution in 15-5PH stainless steel that, in turn, affects its mechanical properties. To investigate the structure–property relationship, the as-built sample and aged samples S1-600 °C-180 min, S2-400 °C-120 min, and S3-500 °C-60 min from the Taguchi array were subjected to microstructure examination. The specimens are selected according to the microhardness results reported in Table 5 as they have the lowest, intermediate, and highest hardness, respectively. The as-built sample in Fig. 2a reveals a typical layered microstructure with well-overlapped molten pools formed by the laser beam. An alternating scan strategy, in which the scanning direction is rotated by 45° between two successive layers, is evident in scan track shapes. The high-magnification SEM image of the as-built sample in Fig. 2b displays equiaxed and columnar sub-grain structures grown epitaxially. The boundaries of the melt pools are apparent by dark lines, and refined equiaxed grains are formed around melt pool boundaries.

In contrast, columnar grains arose parallel to the building direction toward the center of the melt pool. As shown in OM images in Fig. 3, scan track boundaries are eliminated after heat treatment. The heat-treated 15-5PH stainless steel samples represent a more homogenized microstructure. Some defects and porosities can be seen in Figs. 2 and 3. The presence of these flaws is commonly attributed to the

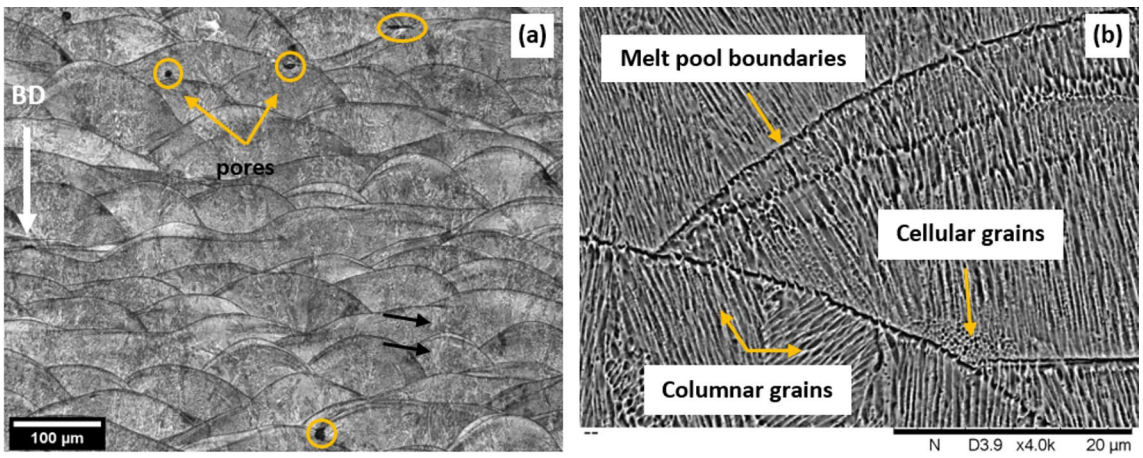

Fig. 2 Microstructure features of as-built 15-5PH stainless steel: **a** optical microscopy and **b** SEM. The black arrows indicate epitaxial growth (color figure online)

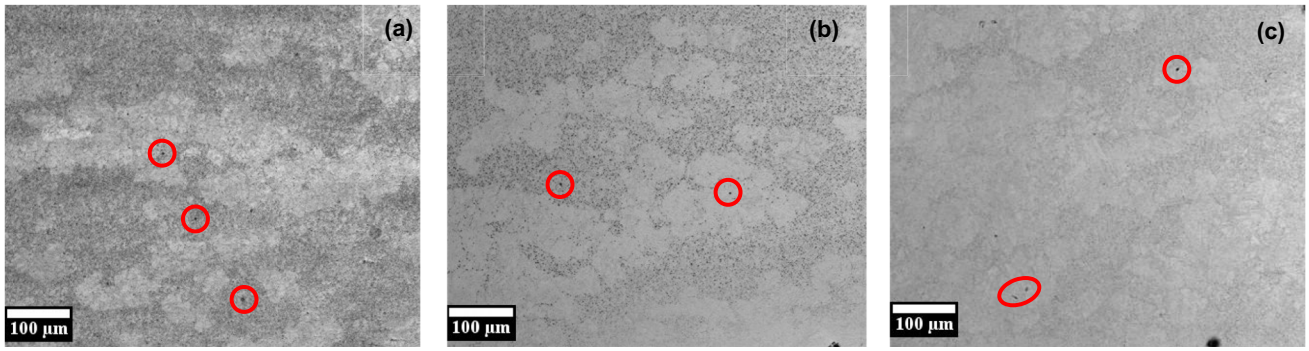

Fig. 3 Optical micrographs of SLM 15-5PH samples after different heat treatments: **a** S1-600 °C-180 min, **b** S2-400 °C-120 min, and **c** S3-500 °C-60 min. The red circles indicate porosities (color figure online)

inadequate melting of the powder and/or the entrapment of gas bubbles [33]. After heat treatment, defects seem to be reduced but not eliminated compared to the as-built specimen. Examining SEM micrographs in Fig. 4 reveals a large proportion of martensite and ferrite phases with retained austenite. The effect of heat treatment on the microstructure of other materials fabricated by SLM has been also reported in previous studies [34, 35].

Although conventional 15-5PH is a martensitic alloy, ferrite and retained austenite in the SLM-processed 15-5PH have been widely reported in the literature [36, 37]. The high cooling rate of the SLM process leads to fine grain size with large strain at the grain boundaries; hence, the austenite retention becomes favorable [38]. The presence of nitrogen in the initial powder may also promote austenite formation. The build chamber temperature during the SLM process may also be greater than the martensite finish temperature, leading to incomplete martensitic transformation [19]. Nong et al. [39] declared that the matrix of the as-built 15-5PH is BCC (martensite and ferrite) with an approximate 10.8% volume fraction of FCC (austenite), which permitted more plastic strain to be accommodated before crack initiation and slowed crack propagation but softened the material.

Since the SLM process has several common points with welding, basically the fast cooling rate, the phase composition of SLM-fabricated 15-5PH stainless steel can be effectively predicted using the Schaeffler diagram, commonly used for welded stainless steel [40]. The effect of austenite and martensite/ferrite stabilizing elements on the microstructure is quantified using the following equations [36]:

$$Ni_{eq}(wt\%) = \%Ni + 30 \times \%C + 30 \times \%N + 0.5 \times \%Mn \quad (1)$$

$$Cr_{eq}(wt\%) = \%Cr + \%Mo + 1.5 \times \%Si + 0.5 \times \%Nb \quad (2)$$

Based on the chemical composition in Table 3, the calculated Ni_{eq} an Cr_{eq} are 15.85% and 8.85%, respectively. The point of intersection is used to predict phase constituents of the 15-5PH microstructure as illustrated in Fig. 5. This point, marked with an orange dot, is worth noting that both the substrate and tensile samples were made of 15-5PH from the substrate using a wire EDM machine, without subsequent heat treatment [7].

After solution treatment of the SLM-fabricated sample, the microstructure transformed into a mostly martensitic matrix with a small residual austenite [41]. During

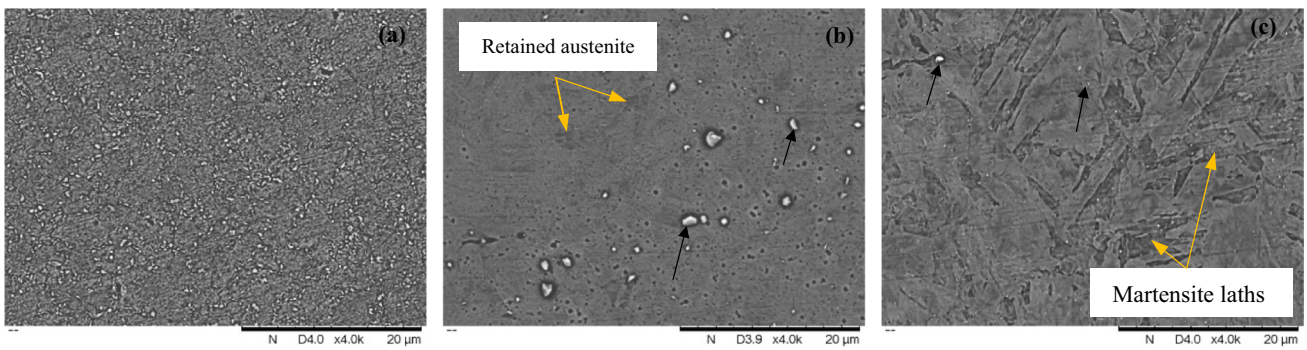

Fig. 4 SEM micrographs of SLM 15-5PH samples after different heat treatments: **a** S1-600 °C-180 min, **b** S2-400 °C-120 min, and **c** S3-500 °C-60 min. Black arrows indicate Cu precipitates (color figure online)

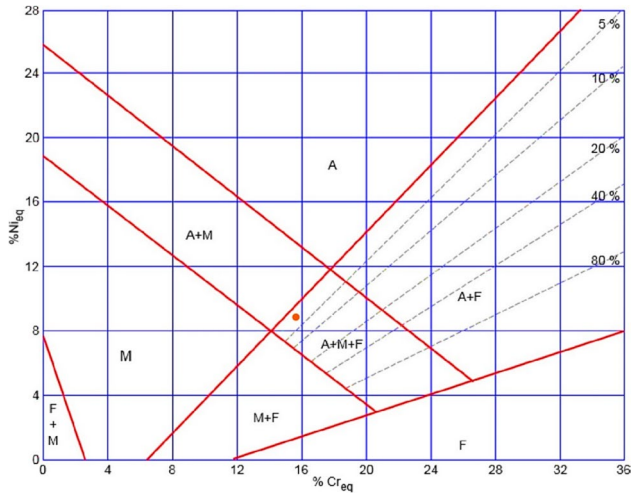

Fig. 5 Schaeffler diagram [7]. The orange dot represents the phase composition of our as-built sample

the subsequent quench, martensite laths grow inside the former austenite grains [10]. Upon aging heat treatment, the second-phase elements, such as copper, are regrouped into clusters by the diffusion process and constitute precipitates.

Figure 4a shows the microstructure of Sample S1-600 °C-80 min, which was aged at 600 °C for 180 min following water quenching. It indicates a heavily tempered martensitic structure and abundant Cu-rich particles with different sizes around the grain boundaries. Figure 4b depicts the microstructure of Sample S2-400 °C-120 min, which was aged at 400 °C for 120 min after being solution-treated and quenched in 6 mass% NaCl solution. The microstructure reveals a higher percentage of austenite than the as-quenched sample (not presented here). This may be explained by the formation of reverted austenite during the aging treatment, as reported by Sarkar et al. [38]. It is also noted that the volume fraction of Cu precipitates is less than that of Sample S1-600 °C-180 min due to the lower aging temperature and aging time. Figure 6 displays the EDS mapping analysis of the second-phase precipitates in Sample S2-400 °C-120 min. It confirms that these were Cu-enriched particles with varying sizes (> 100 nm). Pasebeni reported similar large Cu precipitates non-uniformly distributed in gas-atomized 17-4PH powder produced by SLM following solutionizing and aging at 482 °C. Figure 4c shows the microstructure of Sample S3-500 °C-60 min heat-treated at 500 °C for 60 min after quenching in 12 mass% NaCl solution. It reveals less retained austenite and finer Cu precipitates evenly distributed compared to the two previous samples, which was consistent with the precipitates in traditional 15-5PH stainless steel after similar aging conditions [42]. Some studies have also reported the formation of carbides and nanometric oxide inclusions during the aging of conventional [10, 43] and additively manufactured 15-5PH stainless steel [7, 44] that acted as strengthening factors.

3.2 Microhardness results

Microhardness is a significant mechanical property for metallic components, especially when used in applications that include friction and contact. Microhardness measurements resulting from the various heat treatment combinations are listed in Table 5.

The hardness values range between 36.3 HRC and 46.5 HRC with 39.5 HRC for the as-built specimen. Considering the orthogonal array combinations, Sample S3-500 °C-60 min exhibited the highest hardness, whereas Sample S1-600 °C-180 min exhibited the lowest hardness. The as-quenched samples had the lowest values among all the samples. These findings show good agreement with the literature [7, 38, 45], since our test Sample S3-500 °C-60 min is comparable to the H900 standard aging treatment, which demonstrated the maximum strength and hardness. After being reduced by solution treatment, aging at 400 °C brings back hardness to the as-built value. Further, a rise in temperature to 500 °C induces an increase in hardness by ~ 15% compared to the as-built sample and ~ 24% compared to the as-quenched samples. In contrast, after aging at 600 °C, the hardness values decline again. This variation is correlated to the complex microstructural evolution. The presence of retained and reverted austenite softens the material, while fine Cu-rich precipitates harden it. Primig et al. [12] proved that a significant evolution of 15-5PH chemical composition occurs when aged between 450 and 530 °C, leading to a pronounced hardness peak. Over-aging occurs when the temperature is raised to 600 °C due to the coarsening of copper precipitates [12], and the amount of reverted austenite increases as the heating temperature and duration increase. Consequently, hardness decreases.

3.3 Analysis of variance

ANOVA is a statistical tool that uses the *F* test to investigate which design parameters significantly affect the target response. In this study, ANOVA was performed to assess the significance of each factor in the quench and aging heat treatment process, namely, quenching solution (A), aging temperature (B), and aging time (C), on the hardness of 15-5PH stainless steel parts processed by SLM. The analysis presented in Table 6 is ensured using Minitab 19 statistical analysis software according to the general stepwise method so that only significant factors are kept in the final model. The initial model included independent variables (A, B, C), quadratic variables (A^2, B^2, C^2), and two-way interactions (A × B, A × C, B × C). Statistically significant parameters are determined using the *p* value. Comparing the p value with

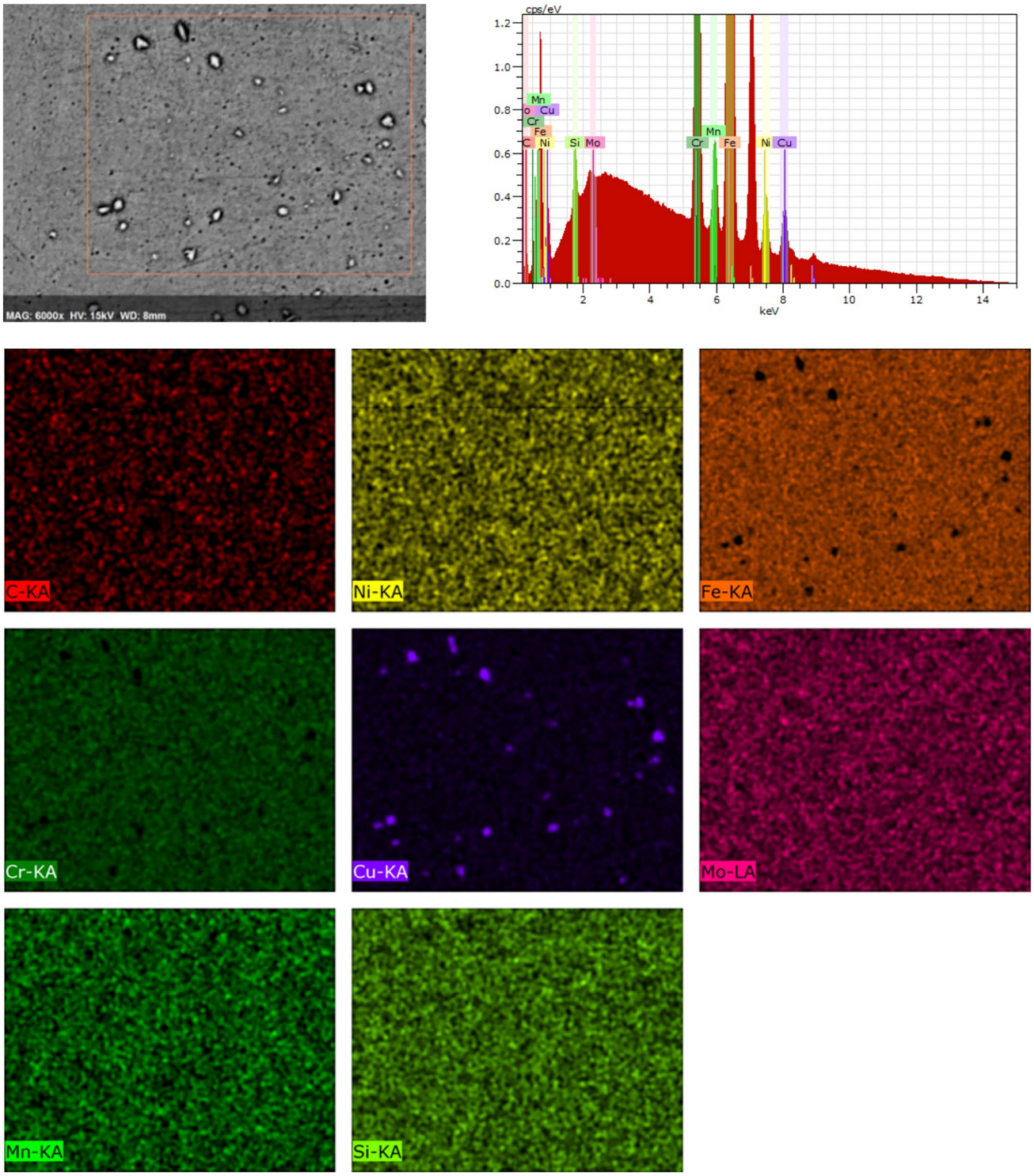

Fig. 6 EDS mapping of Cu precipitates in Sample S2-400 °C-120 min

the fixed significance level (α) determines whether the null hypothesis can be rejected. In this case, the null hypothesis states that the effect of studied parameters is not significant on the hardness of 15-5PH stainless steel produced by SLM. We reject the null hypothesis when the computed p value is less than the designated significance level. In this study, we used a significance level of $\alpha = 0.05$. The percentage contribution is also a rough but effective guide to the relative importance of each model term [46]. An empirical model for hardness as a function of selected variables was developed

Table 6 ANOVA for hardness

Factor	Degree of freedom	Sum of squares	Contribution (%)	Mean squares	*F* value	*p* value
B	1	102.191	5.82	102.191	328.94	0.000
C	1	3.227	2.75	3.227	10.39	0.023
B^2	1	105.609	90.10	105.609	339.94	0.000
Error	5	1.553	1.33	0.311	–	–
Total	8	117.216	100.00	–	–	–

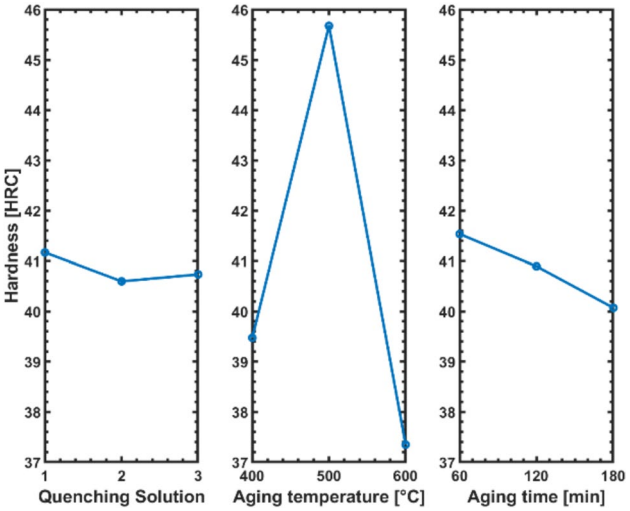

Fig. 7 Main effect plots

by applying linear regression analysis to the experimental data. The general quadratic equation model is stated by [46]:

$$y = \beta_0 + \sum_{i=1}^{3} \beta_i x_i + \sum_{i=1}^{3} \beta_{ii} x_{ii}^2 + \sum_{i=1}^{2} \sum_{j>1}^{3} \beta_{ij} x_i x_j + \varepsilon \quad (3)$$

where y represents the hardness, x_i represent the heat treatment parameters, the β's are regression coefficients, and ϵ is the residual error term. ANOVA results (Table 6) show that hardness is mainly influenced by B^2, B, and C variables. It can be observed that aging temperature (B) is the most influential parameter, accounting for 90.1% of the total variability for the quadratic term B^2 and 5.82% for the linear term B. Aging time (C) is less significant, with a contribution of 2.75%. The quenching solution (A) and the remaining quadratic and interaction terms were omitted from the final model as their p values were much higher than the significance level of $\alpha = 0.05$, meaning that they do not significantly affect the hardness.

To have a better visual perspective of the impact of each heat treatment parameter on the hardness of SLM-fabricated parts, the main effect plots are shown in Fig. 7; aging time hurts hardness. The hardness decrease with prolonged aging time may be ascribed to the coarsening of Cu precipitates and the formation of reverted austenite [47, 48]. The steep variation of mean hardness concerning aging temperature confirms that this factor is highly significant. It has shown a positive effect between 400 and 500 °C and a negative effect between 500 and 600 °C. This variation is in agreement with the chemical and microstructural evolution of 15-5PH stainless steel processed by SLM, which is explained in the microstructure analysis section. The peak hardness was achieved at 500 °C aging temperature due to the uniformly dispersed precipitation of fine Cu precipitates. Lower aging temperature (400 °C) resulted in under-aging characterized by a small volume fraction of Cu precipitates. In comparison, higher aging temperatures led to over-aging, featured by the coarsening of Cu-rich particles and the formation of an extensively reverted austenite phase. Both conditions result in a lower hardness compared to the peak value.

To estimate the hardness of heat-treated SLM parts as a function of the significant factors, a multiple linear regression model was developed using Minitab. The obtained model for predicting hardness is a quadratic model given by Eq. 4.

$$H = -129.2 - 0.01222C + 0.716B - 0.000727B^2 \quad (4)$$

The coefficient of determination R2 that measures the goodness-of-fit of the regression model is 98.6%. In other words, the regression model explains 98.6% of the total variation in hardness. The adjusted R^2 (97.88%) and the predicted R^2 (95.72%) are in reasonable agreement, confirming that the predicted model for hardness can be employed. The standard deviation S of the data values around the fitted values is 0,55, meaning that our model describes the hardness response well.

3.4 Response surface model

The ANOVA results led us to conclude that aging temperature and aging time are the most influential factors in the heat treatment process that affect the hardness of SLM-fabricated 15-5PH components. Further investigation into this relationship allows for estimating the optimal set of parameters that provide the highest hardness. For this purpose, the response surface method (RSM), a statistical technique for modeling

and analysis of such optimization problems, is used. The optimum can be localized with reasonable precision by generating contour plots for response surface analysis. Figures 8 and 9 show the 2D contour plot and the 3D response surface for hardness versus aging time and aging temperature. The variation of hardness as a function of the quenching solution is not considered in the plots since ANOVA results show it to be insignificant. Thus, it is taken as a constant parameter at level 1 since it showed slightly higher hardness according to the main effect plot. It can be inferred from these plots that hardness increases with decreasing holding time. The quadratic relationship between aging temperature and hardness is visible through the parabolic curves of the contour plot. The hardness reaches its maximum when the precipitation hardening temperature ranges between 470 and 515 °C approximately and the aging time ranges between 60 and 80 min. Thus, we can consider 490 °C and 70 min as the best set of parameters for precipitation hardening heat treatment.

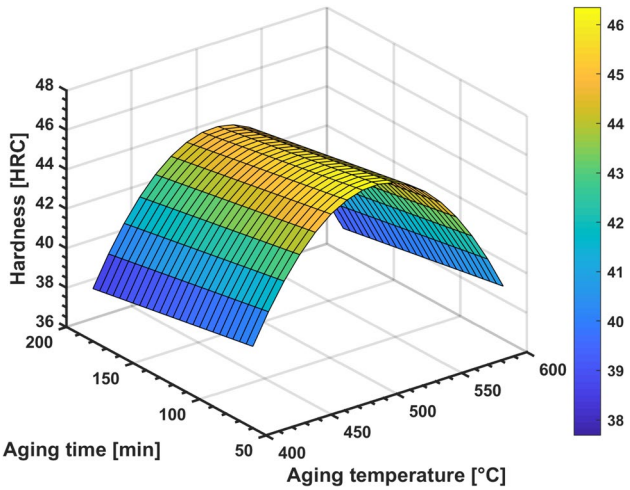

Fig. 9 Three-dimensional response surface plot of hardness versus aging temperature and aging time

3.5 Tensile properties

Both hardness and tensile strength are essential properties of metallic components that are linearly correlated [49]. Achieving maximal hardness implies having the highest tensile strength as well. Therefore, to validate the fitted model and assess the mechanical properties of heat-treated 15-5PH stainless steel produced by SLM, tensile tests were conducted on peak-aged and as-built specimens using MTS-810 tensile testing machine. Precipitation hardening was performed at 490 °C for 70 min after solution treatment and water quenching to obtain the maximum hardness determined by RSM analysis. Two samples for each testing condition are tested, and the mean values of their tensile properties are summarized in Table 7. Figure 10 illustrates the stress–strain curves. The results of tensile tests indicate that precipitation hardening heat treatment has enhanced the mechanical properties of SLM-fabricated 15-5PH

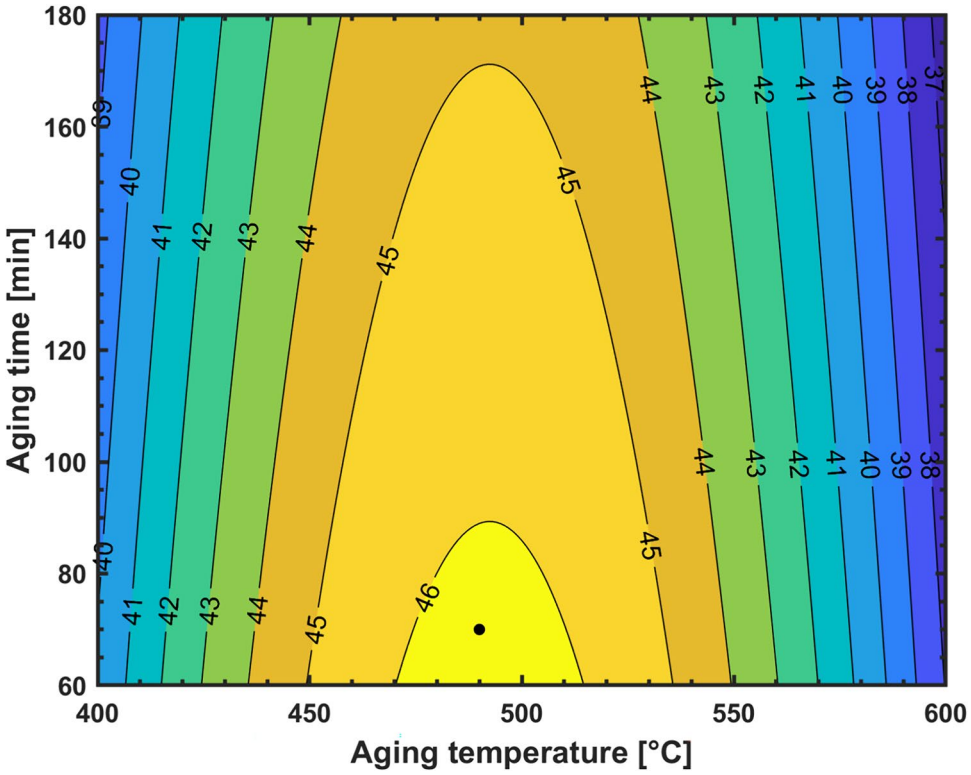

Fig. 8 Two-dimensional contour plot of hardness versus aging temperature and aging time. The black dot represents the optimum point (color figure online)

Table 7 Average tensile properties of 15-5PH stainless steel under as-built and optimal heat-treated conditions

Test	Yield strength (MPa)	Tensile strength (MPa)	Elongation at break (%)
As-built	1190 ± 10	1335 ± 35	4.4 ± 0.165
Heat-treated	1576 ± 11.5	1692 ± 16	8.3 ± 1.01

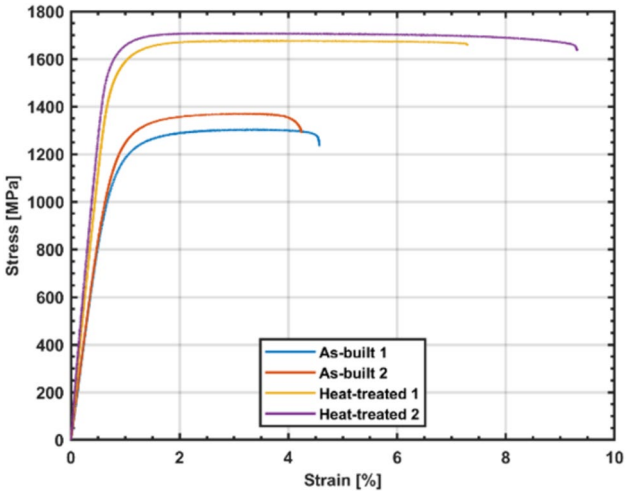

Fig. 10 Stress–strain curves of as-built and peak-aged 15-5PH stainless steel

stainless steel. The yield strength of the heat-treated specimen has increased by approximately 32%, ultimate tensile strength by 26%, and ductility by 89% compared to the as-built specimen. The selected set of parameters enabled the optimal combination of strength, hardness, and ductility to be achieved. This outstanding combination of strength and ductility can be ascribed to (1) grain refinement, (2) high dislocation density, (3) high volume fraction of fine Cu-rich precipitates, and (4) transformation-induced plasticity during tensile deformation due to the presence of retained austenite [44, 47, 50].

4 Conclusion

This work investigates the effect of heat treatment parameters on the hardness and microstructure of selective laser-melted 15-5PH stainless steel. The observation of 15-5PH SS microstructure before and after heat treatment revealed the presence of ferrite, retained/reverted austenite, and copper precipitates. The experimental approach using Taguchi design and analysis of variance (ANOVA) allowed a deep understanding of the influence of quenching solution, aging temperature, and aging time on the hardness of samples. The findings reveal that hardness is mainly affected by aging temperature and less by aging time. Predictive regression and RSM models for hardness were developed using the aforementioned heat treatment parameters as independent variables. The optimal set of parameters was then selected and validated by tensile tests. The validation samples were solution-treated at 1020 °C for 15 min, water-quenched, and aged at 490 °C for 70 min. The resulting mechanical properties are very promising, with higher hardness (up to 46 HRC), higher mechanical strength (ultimate tensile strength up to 1692 MPa), and improved ductility (elongation at break up to 8%) compared to the as-built samples. This can be attributed to the high volume fraction of fine Cu-rich precipitates and transformation-induced plasticity during tensile deformation due to retained austenite. The results of the present study can be used to tailor the mechanical properties of the SLM-fabricated 15-5PH stainless steel by tuning post-process heat treatment parameters. In future works, validation hardness tests and microstructure analysis of the optimal sample obtained from RSM should be given priority. Performing additional tests outside the variation range of parameters presented in this study is needed to improve and assess the accuracy of the predictive model. More in-depth analyses, using more advanced techniques such as high-resolution transmission electron microscopy or atom probe tomography, are also necessary to properly characterize the unique microstructure of SLM-processed 15-5PH stainless steel and investigate the process-structure–property relationship deeply.

Funding The authors did not receive support from any organization for the submitted work.

Declarations

Conflict of interest The authors declare that they have no known competing financial interests or personal relationships that could have appeared to influence the work reported in this paper.

References

1. Brandt M (2017) The role of lasers in additive manufacturing. In: Laser additive manufacturing, p 1–18
2. Katz-Demyanetz A, Popov VV, Kovalevsky A, Safranchik D, Koptyug A (2019) Powder-bed additive manufacturing for aerospace application: techniques, metallic and metal/ceramic composite materials and trends. Manuf Rev 6:5
3. Yap CY, Chua CK, Dong ZL, Liu ZH, Zhang DQ, Loh LE, Sing SL (2015) Review of selective laser melting: materials and applications. Appl Phys Rev 2:41101
4. Mansoura A, Dehghan S, Barka N, Kangranroudi SS (2024) Investigation into the effect of process parameters on density, surface roughness, and mechanical properties of 316L stainless steel fabricated by selective laser melting. Int J Adv Manuf Technol 130:2547–2562

5. Sun S, Brandt M, Easton M (2017) Powder bed fusion processes: an overview. In: Brandt M (ed) Laser additive manufacturing: materials, design, technologies, and applications. Woodhead Publishing, Cambridge, pp 55–77
6. Snow Z, Nassar AR, Reutzel EW (2020) Invited review article: review of the formation and impact of flaws in powder bed fusion additive manufacturing. Addit Manuf 36:101457
7. Unti LFK, Aota LS, Jardini AL, Tschiptschin AP, Sandim HRZ, Jägle EA, Zilnyk KD (2021) Microstructural characterization of 15–5PH stainless steel processed by laser powder-bed fusion. Mater Charact 181:111485
8. Kumar A, Balaji Y, Prasad NE, Gouda G, Tamilmani K (2013) Indigenous development and airworthiness certification of 15-5 PH precipitation hardenable stainless steel for aircraft applications. Sadhana 38:3–23
9. Alafaghani A, Qattawi A, Jaman MS, Ablat MA (2019) Microstructure and mechanical properties of direct metal laser–sintered 15-5PH steel with different solution annealing heat treatments. Int J Adv Manuf Technol 105:3499–3520
10. Couturier L, De Geuser F, Descoins M, Deschamps A (2016) Evolution of the microstructure of a 15-5PH martensitic stainless steel during precipitation hardening heat treatment. Mater Des 107:416–425
11. Peng X, Zhou X, Hua X, Wei Z, Liu H (2015) Effect of aging on hardening behavior of 15-5 PH stainless steel. J Iron Steel Res Int 22:607–614
12. Primig S, Stechauner G, Kozeschnik E (2017) Early stages of Cu precipitation in 15-5 PH maraging steel revisited-part I: experimental analysis. Steel Res Int 88:1600084
13. Habibi Bajguirani HR (2002) The effect of ageing upon the microstructure and mechanical properties of type 15-5 PH stainless steel. Mater Sci Eng A 338:142–159. https://doi.org/10.1016/S0921-5093(02)00062-X
14. Anil Kumar V, Karthikeyan MK, Gupta RK, Gino Prakash F, Ram Kumar P (2012) Aging behavior in 15-5 PH precipitation hardening martensitic stainless steel. In: Materials science forum. Trans Tech Publ, p 483–488
15. Li K, Zhan J, Yang T, To AC, Tan S, Tang Q, Cao H, Murr LE (2022) Homogenization timing effect on microstructure and precipitation strengthening of 17-4PH stainless steel fabricated by laser powder bed fusion. Addit Manuf 52:102672. https://doi.org/10.1016/j.addma.2022.102672
16. Pasebani S, Ghayoor M, Badwe S, Irrinki H, Atre SV (2018) Effects of atomizing media and post processing on mechanical properties of 17-4 PH stainless steel manufactured via selective laser melting. Addit Manuf 22:127–137. https://doi.org/10.1016/j.addma.2018.05.011
17. Yadollahi A, Shamsaei N, Thompson SM, Elwany A, Bian L (2017) Effects of building orientation and heat treatment on fatigue behavior of selective laser melted 17-4 PH stainless steel. Int J Fatigue 94:218–235. https://doi.org/10.1016/j.ijfatigue.2016.03.014
18. Rafi HK, Starr TL, Stucker BE (2013) A comparison of the tensile, fatigue, and fracture behavior of Ti–6Al–4V and 15-5 PH stainless steel parts made by selective laser melting. Int J Adv Manuf Technol 69:1299–1309
19. Coffy K (2014) Microstructure and chemistry evaluation of direct metal laser sintered 15-5 PH stainless steel
20. Roberts D, Zhang Y, Charit I, Zhang J (2018) A comparative study of microstructure and high-temperature mechanical properties of 15-5 PH stainless steel processed via additive manufacturing and traditional manufacturing. Prog Addit Manuf 3:183–190
21. Alafaghani A, Qattawi A, Castañón MAG (2018) Effect of manufacturing parameters on the microstructure and mechanical properties of metal laser sintering parts of precipitate hardenable metals. Int J Adv Manuf Technol 99:2491–2507
22. Wang L, Dong C, Kong D, Man C, Liang J, Wang C, Xiao K, Li X (2020) Effect of manufacturing parameters on the mechanical and corrosion behavior of selective laser-melted 15-5PH stainless steel. Steel Res Int 91:1900447
23. Lass EA, Zhang FAN, Campbell CE (2020) Nitrogen effects in additively manufactured martensitic stainless steels: conventional thermal processing and comparison with wrought. Metall Mater Trans A 51:2318–2332
24. Nong XD, Zhou XL (2021) Effect of scanning strategy on the microstructure, texture, and mechanical properties of 15-5PH stainless steel processed by selective laser melting. Mater Charact 174:111012. https://doi.org/10.1016/j.matchar.2021.111012
25. Nong XD, Zhou XL, Li JH, Wang YD, Zhao YF, Brochu M (2020) Selective laser melting and heat treatment of precipitation hardening stainless steel with a refined microstructure and excellent mechanical properties. Scr Mater 178:7–12. https://doi.org/10.1016/j.scriptamat.2019.10.040
26. Sarkar S, Mukherjee S, Kumar CS, Kumar Nath A (2020) Effects of heat treatment on microstructure, mechanical and corrosion properties of 15-5 PH stainless steel parts built by selective laser melting process. J Manuf Process 50:279–294. https://doi.org/10.1016/j.jmapro.2019.12.048
27. Lee J-R, Lee M-S, Chae H, Lee SY, Na T, Kim W-S, Jun T-S (2020) Effects of building direction and heat treatment on the local mechanical properties of direct metal laser sintered 15-5 PH stainless steel. Mater Charact 167:110468. https://doi.org/10.1016/j.matchar.2020.110468
28. Wang L, Dong C, Man C, Kong D, Xiao K, Li X (2020) Enhancing the corrosion resistance of selective laser melted 15-5PH martensite stainless steel via heat treatment. Corros Sci 166:108427. https://doi.org/10.1016/j.corsci.2019.108427
29. Kultz Unti LF, Aota LS, Jardini AL, Tschiptschin AP, Sandim HRZ, Jägle EA, Zilnyk KD (2021) Microstructural characterization of 15-5PH stainless steel processed by laser powder-bed fusion. Mater Charact 181:111485. https://doi.org/10.1016/j.matchar.2021.111485
30. Yang WH, Tarng YS (1998) Design optimization of cutting parameters for turning operations based on the Taguchi method. J Mater Process Technol 84:122–129
31. Agboola OO, Ikubanni PP, Adeleke AA, Adediran AA, Adesina OS, Aliyu SJ, Olabamiji TS (2020) Optimization of heat treatment parameters of medium carbon steel quenched in different media using Taguchi method and grey relational analysis. Heliyon 6:e04444
32. Zordão LHP, Oliveira VA, Totten GE, Canale LCF (2019) Quenching power of aqueous salt solution. Int J Heat Mass Transf 140:807–818
33. Mansoura A, Omidi N, Barka N, Kangranroudi SS, Dehghan S (2024) Selective laser melting of stainless steels: a review of process, microstructure and properties. Metals Mater Int. https://doi.org/10.1007/s12540-024-01650-8
34. Waqas M, He D, Liu Y, Riaz S, Afzal F (2023) Effect of heat treatment on microstructure and mechanical properties of Ti_6Al_4V alloy fabricated by selective laser melting. J Mater Eng Perform 32:680–694
35. Yan X, Yin S, Chen C, Huang C, Bolot R, Lupoi R, Kuang M, Ma W, Coddet C, Liao H (2018) Effect of heat treatment on the phase transformation and mechanical properties of Ti_6Al_4V fabricated by selective laser melting. J Alloys Compd 764:1056–1071
36. Lee J-R, Lee M-S, Chae H, Lee SY, Na T, Kim W-S, Jun T-S (2020) Effects of building direction and heat treatment on the local mechanical properties of direct metal laser sintered 15-5 PH stainless steel. Mater Charact 167:110468
37. Contaldi V, Del Re F, Palumbo B, Squillace A, Corrado P, Di Petta P (2019) Mechanical characterisation of stainless steel parts

produced by direct metal laser sintering with virgin and reused powder. Int J Adv Manuf Technol 105:3337–3351
38. Sarkar S, Kumar CS, Nath AK (2019) Effects of heat treatment and build orientations on the fatigue life of selective laser melted 15-5 PH stainless steel. Mater Sci Eng, A 755:235–245
39. Nong XD, Zhou XL, Li JH, Wang YD, Zhao YF, Brochu M (2020) Selective laser melting and heat treatment of precipitation hardening stainless steel with a refined microstructure and excellent mechanical properties. Scr Mater 178:7–12
40. Jacob G, Jacob G (2018) Prediction of solidification phases in Cr–Ni stainless steel alloys manufactured by laser based powder bed fusion process. US Department of Commerce, National Institute of Standards and Technology
41. Wang L, Dong C, Man C, Kong D, Xiao K, Li X (2020) Enhancing the corrosion resistance of selective laser melted 15-5PH martensite stainless steel via heat treatment. Corros Sci 166:108427
42. Luo H, Yu Q, Dong C, Sha G, Liu Z, Liang J, Wang L, Han G, Li X (2018) Influence of the aging time on the microstructure and electrochemical behaviour of a 15-5PH ultra-high strength stainless steel. Corros Sci 139:185–196
43. Bajguirani HRH (2002) The effect of ageing upon the microstructure and mechanical properties of type 15-5 PH stainless steel. Mater Sci Eng A 338:142–159
44. Chae H, Luo MY, Huang E-W, Shin E, Do C, Hong S-K, Woo W, Lee SY (2022) Unearthing principal strengthening factors tuning the additive manufactured 15-5 PH stainless steel. Mater Charact 184:111645
45. LeBrun T, Nakamoto T, Horikawa K, Kobayashi H (2015) Effect of retained austenite on subsequent thermal processing and resultant mechanical properties of selective laser melted 17-4 PH stainless steel. Mater Des 81:44–53
46. Montgomery DC (2017) Design and analysis of experiments. John wiley & sons, Hoboken
47. Sabooni S, Chabok A, Feng SC, Blaauw H, Pijper TC, Yang HJ, Pei YT (2021) Laser powder bed fusion of 17-4 PH stainless steel: a comparative study on the effect of heat treatment on the microstructure evolution and mechanical properties. Addit Manuf 46:102176
48. Hsiao CN, Chiou CS, Yang JR (2002) Aging reactions in a 17-4 PH stainless steel. Mater Chem Phys 74:134–142
49. Pavlina EJ, Van Tyne CJ (2008) Correlation of yield strength and tensile strength with hardness for steels. J Mater Eng Perform 17:888–893
50. Chae H, Huang E-W, Jain J, Wang H, Woo W, Chen S-W, Harjo S, Kawasaki T, Lee SY (2019) Plastic anisotropy and deformation-induced phase transformation of additive manufactured stainless steel. Mater Sci Eng, A 762:138065